

2019

Biosensor for the oxidative stress biomarker glutathione based on SAM of cobalt phthalocyanine on a thioctic acid modified gold electrode

Mohammed Nooredeen Abbas

National Research Centre, Dokki, Cairo, Egypt, dr.noorscientist@gmail.com

Ayman Ali Saeed

National Research Centre, Dokki, Cairo, Egypt

Mounir Ben Ali

Université de Sousse, Tunisia

See next page for additional authors

Follow this and additional works at: <https://arrow.tudublin.ie/ittsciart>

 Part of the [Chemistry Commons](#)

Recommended Citation

Abbas, M.N., Saeed, A.A., Ali, M.B. et al. Biosensor for the oxidative stress biomarker glutathione based on SAM of cobalt phthalocyanine on a thioctic acid modified gold electrode. *J Solid State Electrochem* 23, 1129–1144 (2019). DOI: 10.1007/s10008-018-04191-4

This Article is brought to you for free and open access by the School of Science and Computing at ARROW@TU Dublin. It has been accepted for inclusion in Articles by an authorized administrator of ARROW@TU Dublin. For more information, please contact arrow.admin@tudublin.ie, aisling.coyne@tudublin.ie, gerard.connolly@tudublin.ie.



This work is licensed under a [Creative Commons Attribution-NonCommercial-Share Alike 4.0 License](#)
Funder: EU - FP7 Marie Curie IRSES Project

Authors

Mohammed Nooredeen Abbas, Ayman Ali Saeed, Mounir Ben Ali, Abdelhamid Errachid, Nadia Zine, Abdullatif Baraket, and Baljit Singh



Biosensor for the oxidative stress biomarker glutathione based on SAM of cobalt phthalocyanine on a thioctic acid modified gold electrode

Mohammed Nooredeen Abbas¹ · Ayman Ali Saeed¹ · Mounir Ben Ali² · Abdelhamid Errachid³ · Nadia Zine³ · Abdullatif Baraket³ · Baljit Singh⁴

Received: 16 April 2018 / Revised: 29 November 2018 / Accepted: 30 December 2018 / Published online: 8 February 2019
© Springer-Verlag GmbH Germany, part of Springer Nature 2019

Abstract

Self-assembled monolayer (SAM) of cobalt teraaminophthalocyanine (CoTAPc) was developed on thioctic acid (TA) dithiol modified gold electrode and electrochemically evaluated as a glutathione (GSH) selective biosensor. The CoTAPc-TA-Au modified electrode was developed by the covalent immobilization of the CoTAPc as the electrochemical mediator onto previously prepared gold electrode modified with TA (TA-Au) via amid bond formation with the carboxylic group of TA, producing well-organized SAM of the mediator. For comparison, another electrode modified with 3-mercaptopropionic acid (MPA) as a monothiol linker instead of TA was similarly prepared. The electrode surface modification was characterized using SEM, AFM, CV, and EIS. The contact angle measurements of the surface confirmed the formation of CoTAPc SAM on both TA and MPA modified electrodes. The CoTAPc-TA-Au modified electrode showed enhanced catalytic activity for GSH oxidation compared to that of CoTAPc-MPA-Au, indicating that the TA dithiol allowed for more coverage of the catalyst layer on the electrode surface with stronger binding. The experimental parameters controlling the voltammetric processes like scan rate and pH of sample solution were optimized. Using DPV technique, the proposed sensor exhibited a linear response of oxidation peak current vs. GSH concentration, over the concentration range between 10 and 100 $\mu\text{mol L}^{-1}$ with a LOD of 1.5 $\mu\text{mol L}^{-1}$ for the CoTAPc-TA-Au modified electrode compared to 5.5 $\mu\text{mol L}^{-1}$ GSH, for the CoTAPc-MPA-Au electrode. The proposed sensor was utilized for detection of glutathione in some hemolyzed blood samples.

Keywords Glutathione · Biosensor · SAM · Thioctic acid · Cobalt phthalocyanine

Electronic supplementary material The online version of this article (<https://doi.org/10.1007/s10008-018-04191-4>) contains supplementary material, which is available to authorized users.

✉ Mohammed Nooredeen Abbas
dr.noorscientist@gmail.com

¹ Electroanal. Lab., Applied Organic Chemistry Department, National Research Centre (NRC), El Bohouth St., Dokki, Giza 12622, Egypt

² Université de Sousse, ISSAT de Sousse, Cité Ettafala, 4003 Ibn Khaldoun Sousse, Tunisia

³ Institut des Sciences Analytiques (ISA), Université de Lyon, Université de Claude Bernard Lyon 1, UMR 5280, 5 rue de la Doua, 69100 Villeurbanne, France

⁴ MiCRA Biodiagnostics Technology Gateway, Institute of Technology Tallaght, Dublin 24 D24 FKT9, Ireland

Introduction

The tripeptide glutathione (GSH) is a critical physiological component endogenous to all biological tissues and fluids [1, 2]. This tripeptide containing a sulfhydryl group plays important biological functions in the living organism, including protein and DNA synthesis, enzyme activity, metabolism, and cell protection. Reduced glutathione (GSH) (γ -L-glutamyl-L-cysteinyglycine) is the major non-protein thiol in living cells, with cellular concentrations ranging from 0.5 to 10 mmol L^{-1} . It is considered as one of the most important agents of the antioxidant defense system of the cell. In conjunction with the enzymes glutathione peroxidase (GSH-Px) and glutathione S transferase pi (GSTpi), it plays a central role in the detoxification and biotransformation of chemotherapeutic drugs [3]. Existing primarily in its reduced form, an overproduction of reactive oxygen species (ROS) initiates the conversion of GSH to its corresponding disulphide (GSSG) [2, 4,

5]. An alteration in the level of GSH or the GSH/GSSG ratio is one of the first indications of cellular oxidative stress, a status which has been implicated in the pathophysiology of conditions such as Alzheimer's, Parkinson's and Huntington's disease [4, 5]. GSH and its oxidized forms, glutathione disulphide (GSSG) and glutathionylated proteins (PSSG) are considered as biomarkers [6] of oxidative stress. Autism is an increasingly prevalent neurodevelopmental disorder in the United States, which relies on applied behavioral therapy as means of treatment. This disorder has been linked to increased levels of oxidative stress and lower antioxidant capacity. Metabolites in the interconnected transmethylation and transsulfuration pathways are significantly altered in autism, causing decreased glutathione synthesis. The use of the glutathione redox ratio as a biomarker for disease and treatment status was supported by several reports [7]. In addition, a high burden of oxidative stress, quantified by the plasma amino thiols, cystine, glutathione, and their ratio, is associated with mortality [8] in patients with coronary artery disease, a finding that is independent of and additive to the inflammatory burden. Therefore, this tripeptide was established to be a biomarker of oxidative stress and its concentration in blood can be relevant for the clinical diagnosis. Analytical methodologies to determine GSH often involve complex sample pretreatment steps such as derivatization of the analyte for fluorescence detection [9]. However, direct methods such as electrochemical [10] and chemiluminescence [11] are simpler. Electrochemical methods using modified electrodes offer simple, sensitive and selective analytical alternative. Chemically modified electrodes (CMEs) have continued to be of major concern during the past decade and a relatively large amount of electrochemical research has been devoted to the development and applications of different types of CMEs. Modification of the electrode surface, especially a gold electrode with a self-assembled monolayer (SAMs) of alkane thiols or their derivatives has been well studied, being of considerable interest in the field of electroanalysis and biosensor development. SAMs on gold have also been shown to be useful for the chemical immobilization of redox mediators [12, 13], enzymes, and antibodies for biosensor development [14, 15]. The stability of a SAM modified gold electrode is related to the fact that the alkane thiol reacts strongly with gold to form a bond with covalent character [16]. As a sulfur-containing compound, thioctic acid (TA) has received great attention in the area of gold surface functionalization for a number of reasons: the alkyl chain length in TA would be expected to result in a more ordered SAM than a simple mercaptoalkyl ether, and disulphide attachment to gold surfaces results in enhanced stability. Therefore, TA was employed as a linker for the attachment of lipids, carbohydrates, proteins, and oligonucleotides to gold surfaces [17, 18]. At the same time, it is now well known that certain transition metal complexes with phthalocyanines [19],

porphyrins, Schiff bases, and other ligands can catalyze, via reduction of their central metal ions, the electro-oxidation of several important chemical and biological compounds. A number of these compounds, as mediators in modified electrodes, have been characterized for electrocatalysis of some sulfhydryl compounds such as cysteine and its derivatives, glutathione, 2-mercaptoethanol and other sulfhydryl compounds. FePc modified-AuNPS composite in a CPE has been successfully utilized for the catalytic oxidation of cysteine [20]. Covalent attachment of redox mediators to the surface of the monolayer containing some free terminal groups like COOH and NH₂ through amide linkage formation provides a well ordering of these mediators on the surface of the electrode which also affects the rate of electron transfer processes. Cobalt (II) phthalocyanine [21] is well reported as an excellent electro-catalyst for the enhancement of the oxidation of glutathione. Different electrodes with different CoPc immobilization techniques were reported for glutathione detection. Adsorption of CoPc on pyrolytic graphite electrode [22], immobilization on nitrogen-doped graphene [23], Covalent attachment to graphene oxide [24], intercalation with Zn–Al layered double hydroxide [25] or as a composite in modified screen printed electrodes [26, 27] are among the different techniques used. In this paper, we aimed at developing a SAM modified gold electrode with SAM of cobalt tetraaminophthalocyanine (CoTAPc) as a glutathione sensor. Gold electrode modified with a monolayer of TA, has been used for the formation of a SAM of CoTAPc, through amide bond formation between its free carboxyl groups and the amino groups of the phthalocyanine molecule. The use of dithiol TA as a linker rather than a monothiol, for the immobilization of the CoTAPc molecules produced well organized monolayer that exhibited excellent electrochemical performance. The strong interaction between the two sulfur atoms of each TA molecule and the gold electrode enabled the formation of stable enough to SAM layer, which prolonged the life time of the immobilized CoTAPc layer resulting in longer life time of the glutathione sensor. The modified electrode was investigated as a biosensor to detect the oxidative stress biomarker glutathione in hemolyzed blood samples.

Experimental

Materials

Gold electrodes SiO₂/Si/SiO₂/Ti/Au (0.3 cm²) were used as working electrodes; Potassium hexacyanoferrate(III) (> 99%), potassium hexacyanoferrate(II) trihydrate (> 99.99%), (±)-α-thioctic acid (TA), 3-mercaptopropionic acid (MPA), L-glutathione reduced (GSH), N-Hydroxysuccinimide (NHS), N-(3-Dimethylaminopropyl)-N'-ethylcarbodiimide hydrochloride (EDC), and 5-sulfosalicylic acid were purchased

from Sigma-Aldrich. 4-nitrophthalic anhydride was purchased from Fluka. Phosphate buffer solution was prepared at pH 7.4 using $0.1 \text{ mol L}^{-1} \text{ KH}_2\text{PO}_4$ and $0.1 \text{ mol L}^{-1} \text{ K}_2\text{HPO}_4$.

Instrumentation

The electrochemical experiments (cyclic voltammetry, electrochemical impedance spectroscopy, and differential pulse voltammetry) were performed using an electrochemical workstation Model 660D, CH Instruments Inc. The experiments were carried out in $5 \text{ mmol L}^{-1} [\text{Fe}(\text{CN})_6]^{3-/4-}$ solution as redox indicating probe and phosphate buffer solution (0.1 mol L^{-1} , pH 7.4). A conventional three-electrode cell equipped with platinum wire and a standard Ag/AgCl electrode (filled with $3 \text{ mol L}^{-1} \text{ KCl}$ solution) as the counter and reference electrodes, respectively, was used. Contact angle (CAM) measurements were performed using Easydrop Model OCA 20, Data Physics Instruments (Germany). The surface morphology was characterized using scanning electron microscopy JEOL JXA-840A. AFM Images were obtained using scanning probe microscope SHIMADZU SPM 9600. X-ray photoelectron spectroscopy (XPS) was performed using Kratos Ultra DLD, using Mono Al X-rays ($K\alpha$ 1486.58 eV; 150 W). Survey and high-resolution (narrow regions) spectra were taken at pass energy of 160 eV and 20 eV respectively. C 1 s peak at 284.8 eV was used as a charge reference to determine core level binding energies. Spectra were collected in the normal to the surface direction. For quantitative analysis, survey spectra were acquired at normal emission (take off angle 90°) and both survey and high-resolution spectra were acquired at a sample tilt of 60° (take off angle 30°). Construction and peak fitting of synthetic peaks in narrow region spectra used a Shirley type background and the synthetic peaks were of a mixed Gaussian-Lorentzian type. Relative sensitivity factors used are from CasaXPS library containing Scofield cross-sections [28].

Synthesis of cobalt (II) tetranitro-phthalocyanine and cobalt (II) tetraamino-phthalocyanine

The synthesis of electro-catalyst was carried out according to the previously reported method [29]. Briefly, 7.72 g of 4-Nitrophthalic anhydride (0.04 mol), 2.49 g of cobalt (II) acetate tetrahydrate (0.01 mol), 25 g of urea, and 0.01 g of ammonium molybdate tetrahydrate as a catalyst were added into 30 mL nitrobenzene, and refluxed at 200°C with stirring for almost 5 h until a stable dark blue color formed. The solvent was excluded by filtration using a G4 glass filter. The precipitate was washed with ethanol, $1.0 \text{ mol L}^{-1} \text{ HCl}$ then $1.0 \text{ mol L}^{-1} \text{ NaOH}$ till a colorless filtrate was observed. The reduction of Co(II)TNPC to Co(II)TAPC was carried out by adding 1 g of Co(II)TNPC and 5 g of sodium sulfide in

50 mL distilled water. The mixture was heated at 50°C with stirring for 5 h. The product was filtered and washed with distilled water till a colorless filtrate. The final structure of the product is shown in Fig. 1.

Gold substrate pretreatment

Before use, the working gold electrodes were sonicated twice in acetone for 10 min, then the electrodes were immersed in Piranha solution (1:3 v/v, 30% H_2O_2 : Conc. H_2SO_4) for 1 min and rinsed thoroughly with water. The cleanliness of the electrode surfaces was ascertained by recording the cyclic voltammogram of the cleaned surface in $5 \text{ mmol L}^{-1} [\text{Fe}(\text{CN})_6]^{3-/4-}$ in $0.1 \text{ mol L}^{-1} \text{ KCl}$ solution.

Formation of CoTAPc SAM on the gold electrode and coupling

The best SAM are formed using a process similar to that used for carboxyl terminated alkyl-thiols by adding acetic acid to ethanol solutions to form and rinse films [30]. The thioctic acid monolayers adsorbed on Au builds a foundation for the use of these films in biological and chemical sensor applications and for surface-attached macromolecules. Modification of the gold electrode with thioctic acid and CoTAPc was done by modifying the previously reported method [31], by dipping the surface in an ethanolic solution of $10^{-2} \text{ mol L}^{-1}$ TA containing 5% acetic acid for 24 h. EDC/NHS coupling reaction was performed to form the amide bond between the amino group in CoTAPc and the carboxylic group of TA monolayer [32] by dipping the electrode in $10^{-2} \text{ mol L}^{-1}$ solution of each of CoTAPc, EDC and NHS in 5 mL of Et OH /DMF (1:1) for 24 h. Finally, the weakly adsorbed or non-adsorbed species were removed by rinsing the modified electrode in Et OH /DMF. Scheme 1 shows a presentation of the formed CoTAPc SAM on the gold electrode.

Real sample preparation

To investigate the applicability of the proposed electrochemical sensor for the electrocatalytic determination of GSH in real

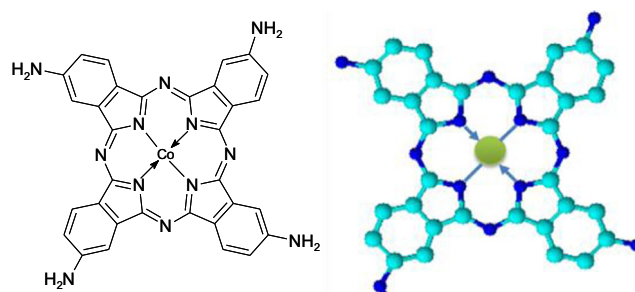
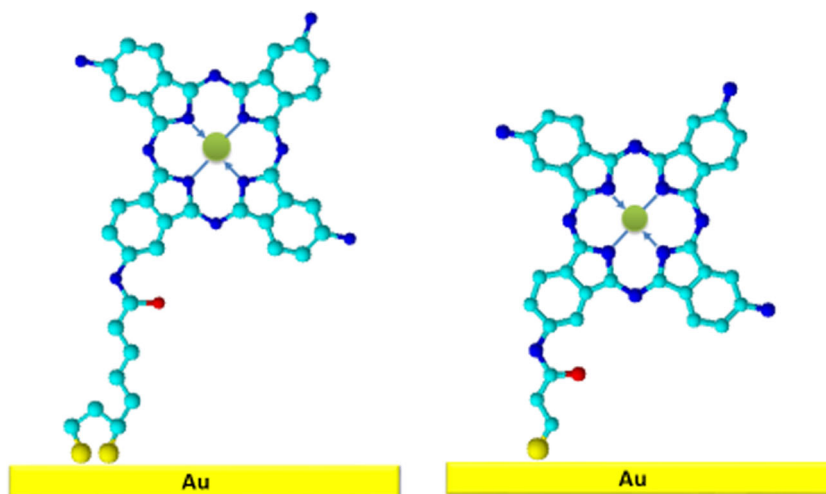


Fig. 1 Cobalt (II)-2,9,16,23-tetraaminophthalocyanine

Scheme 1 Schematic presentation of CoTAPc-TA-Au and CoTAPc-MPA-Au modified electrodes



samples, we selected human blood for the analysis of GSH contents. Human blood was obtained from two volunteers. The erythrocytes contents were separated from the whole blood by discarding the plasma of a 5-mL blood sample by centrifugation for at 3000 rpm. The supernatant was removed and the rest was washed three times with 5 mL of 0.9% NaCl solution. The erythrocyte pellets were hemolyzed with water (1:1 *v/v*). For protein precipitation, the hemolysate was mixed with 5-sulfosalicylic acid (10%, *w/v*) in the ratio of 2:1 (*v/v*). This mixture was centrifuged. Then, the supernatant became ready for the electrochemical determination of glutathione.

Results and discussion

Surface characterizations

Scanning electron microscopy

A scanning electron microscope (SEM) scans a focused electron beam over a surface to create an image. The electrons in the beam interact with the sample, producing various signals that can be used to obtain information about the surface topography and composition. It allows users to examine

specimen at a high resolution. As seen in Fig. 2, the SEM image of bare gold electrode shows no surface features (Fig. 2(a)) in contrast to CoTAPc-TA-Au modified electrode which shows distinct surface protrusions (Fig. 2(b, c)) which is an indication for the success of the assembly and coupling processes.

Atomic force microscopy

Atomic force microscopy (AFM) or scanning force Microscopy (SFM) is a very-high-resolution type of scanning probe microscopy (SPM), with demonstrated resolution on the order of fractions of a nanometer, more than 1000 times better than the optical diffraction limit. Atomic Force Microscopes (AFMs) give us a window into this nanoscale world. AFM has enabled us to deepen our study of film formation and optimize some parameters of deposition protocols. Figure 3(A) (a, b, and c) shows the plane AFM images of the CoTAPc-TA-Au, CoTAPc-MPA-Au and the bare Au gold electrodes, treated for 5 μm . This image shows the effectiveness of cleaning protocol for the bare gold electrode with the piranha solution. Figure 3(B) (a and b) shows 3-D images for the two modified electrodes using TA and MPA thiols with a clear difference in surface morphology. The AFM images show the surface mean

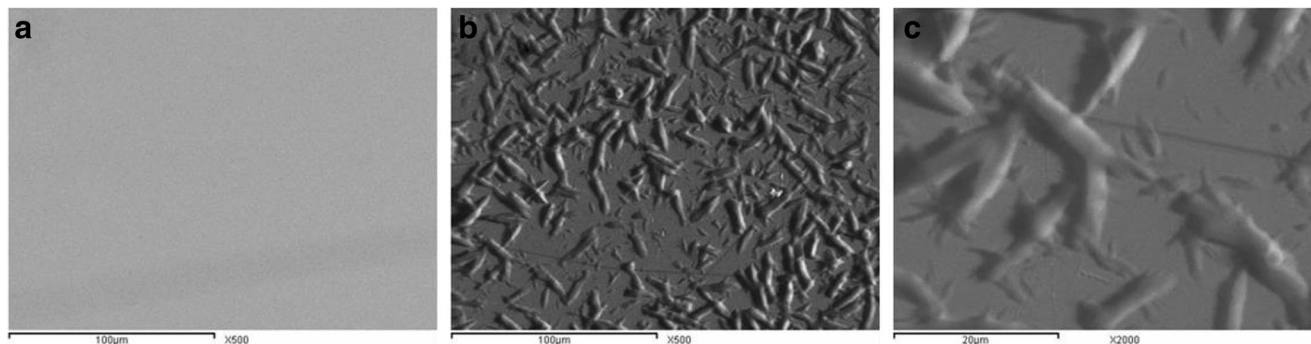


Fig. 2 SEM images of (a) bare gold electrode; (b) CoTAPc-TA-Au modified electrode $\times 500$ and (c) with $\times 2000$ magnification

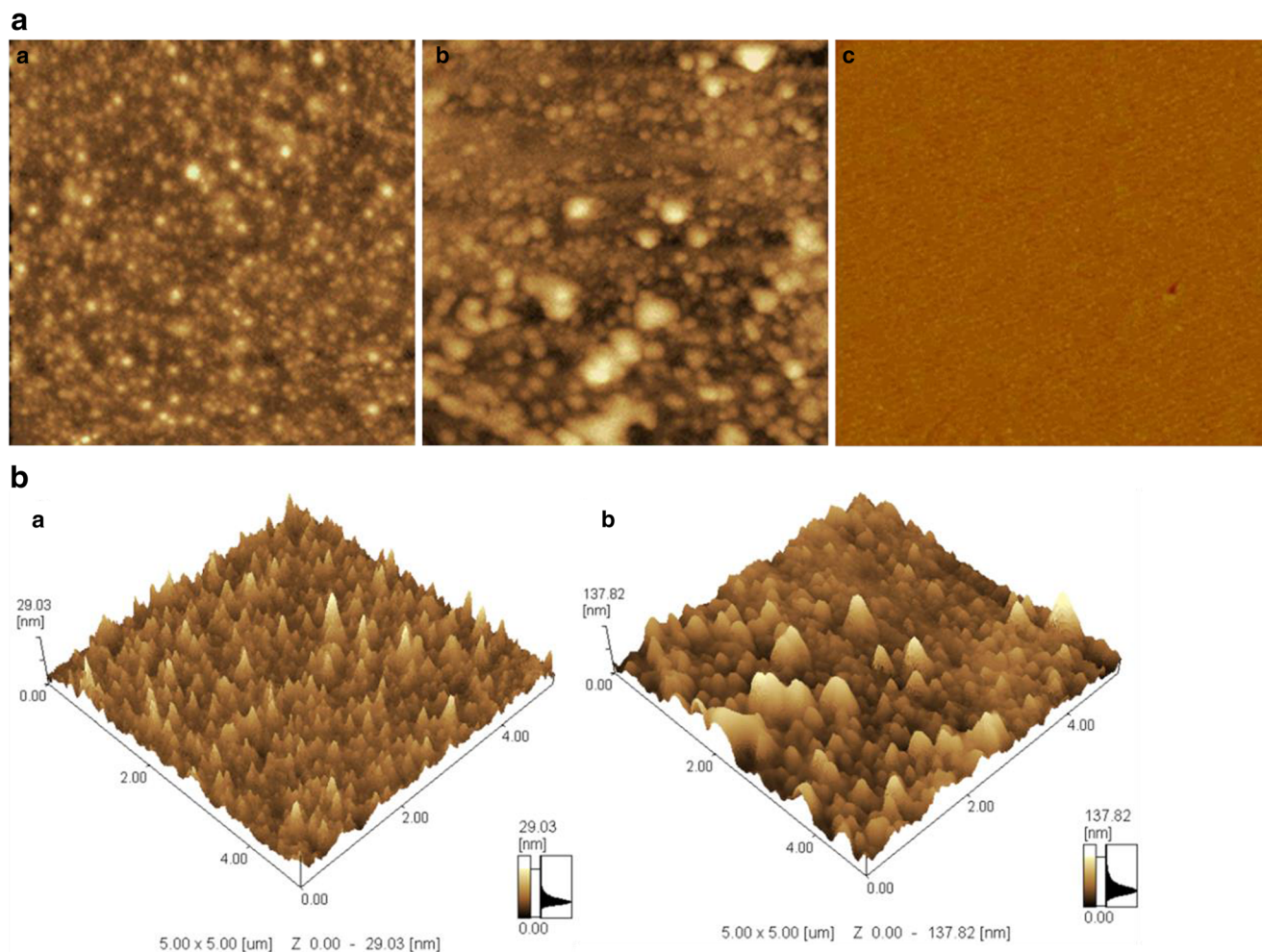


Fig. 3 AFM images (A) plane of (a) CoTAPc-TA-Au, (b) CoTAPc-MPA-Au, and (c) bare Au and (B) 3-D (a) CoTAPc-TA-Au, (b) CoTAPc-MPA-Au

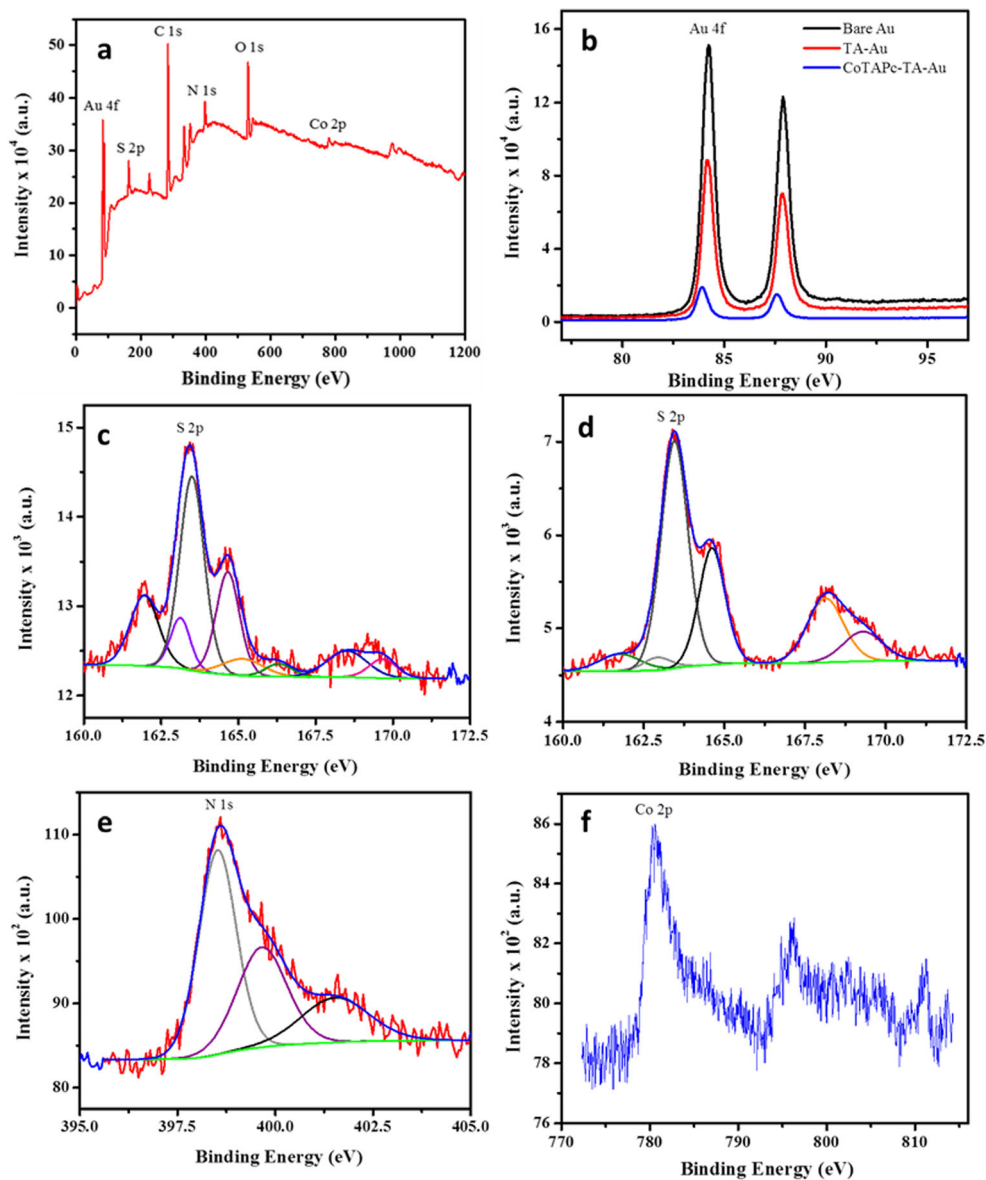
roughness factor values of 29.03 nm for CoTAPc-TA-Au and 137.82 nm for CoTAPc-MPA-Au, compared to the unmodified gold with the mean roughness of 0.54 nm. The increase in roughness factor might be due that various areas of the surface is covered by SAMs while other areas are exposed (as predicted by impedance spectroscopy), thus increasing the mean roughness of the surface.

X-ray photoelectron spectroscopy analysis

In order to confirm the presence of elements, various functional groups and surface composition for the bare and modified gold electrodes, XPS analysis was performed. Figure 4 and S1 summarize the XPS results for each stage of surface modification (TA-Au and CoTAPc-TA-Au) in addition to the bare gold electrode. The survey XPS spectra of bare electrode (Fig. S1a) shows the presence of Au 4f (83.4 eV) which is obvious and due to the gold surface. Au 4f (83.2 eV) and S 2p (163.2 eV) peaks were observed for thioctic acid modified gold electrode (TA-Au, Fig. S1b) which confirm the successful assembly of TA onto the gold electrode via Au-S

interactions. The survey (Fig. 4(a)) and high-resolution spectra for CoTAPc-TA-Au confirm the presence of Au 4f (83.3 eV), S 2p (163.3 eV), N 1s (398.3 eV) and Co 2p (780.6 eV) which are in agreement with the expected surface composition. Overall, the presence of Au, S, N, and Co peaks collectively confirms the successful immobilization of CoTAPc onto the thioctic acid (TA) modified gold electrode [28, 33, 34]. From the high-resolution spectra (Fig. 4(c and d)), S was observed in the form of different functional groups (RS^- , S and $-\text{SH}$) which are associated with the successful assembly of thioctic acid onto the gold surface. The presence of carbon functional groups (C-C, C-O, C=O, O=C-O) and in particular C-N peak at 399.7 eV (Fig. 4(e)) which is only observed for CoTAPc-TA modified gold electrode is a confirmation of phthalocyanine ring. From the high-resolution spectra for CoTAPc-TA modified gold electrode (Fig. 4(f)), Co was found to be in (+2, Co^{2+}) oxidation state and associated with Co-phthalocyanine [28, 33, 34]. In addition, from the high-resolution XPS spectra (Fig. 4(b)), Au 4f shows doublet peaks with narrow FWHM (0.7 eV) at around 84.0 ± 0.2 eV which corresponds to metallic Au [28, 33, 34]. From the

Fig. 4 (a) The survey spectra of CoTAPc-TA modified gold electrode; (b) High-resolution spectra of Au 4f for bare and modified electrodes (labeled); (c and d) High-resolution spectra of S 2p for TA-Au and CoTAPc-TA-Au, respectively; High-resolution spectra of (e) N 1s and (f) Co 2p for CoTAPc-TA-Au








survey spectra analysis, the Au content (surface composition) was found to be 34.3%, 22.6% and 2.6% for bare Au, TA-Au and CoTAPc-TA-Au, respectively. It is clearly evident from the XPS analysis that the surface Au content was reduced by about 66% for TA and 75% for CoTAPc-TA modified gold surfaces compared to the bare gold electrode. This confirms the success of the linker (TA) assembly onto the bare Au surface and CoTAPc immobilization onto the TA modified gold electrode.

Wettability, contact angle measurements

When an interface exists between a liquid and a solid, the angle between the surface of the liquid and the outline of the contact surface is described as the contact angle (θ). The contact angle (wetting angle) is a measure of the

wettability of a solid by a liquid. Wettability measurements were performed to investigate the gold surface quality. Firstly, 5 μL of DI water was deposited onto the surface. Afterwards, the water droplet behavior obtained on the surface was acquired with a digital camera. The wettability was recorded before and after surface modification. Table 1 shows the change of the contact angle as a function of the modification performed on the gold surface. In the first step, the gold surface was cleaned well with acetone and piranha and the contact angle was measured at 67.2°. This value shows the hydrophilic properties of the surface. In the second step, the thiol was allowed to assemble onto the surface. The contact angle after assembly of thioctic acid and 3-mercaptopropionic acid was 62.0° and 35.6°, respectively. This attributed to the fact that thiol has a carboxylic group, and a

Table 1 Contact angle measurements

Surface composition	CA, θ	Droplet shape
Bare gold	$67.2^\circ \pm 1^\circ$	
MPA-Au	$35.6^\circ \pm 1^\circ$	
TA-Au	$62.0^\circ \pm 1^\circ$	
CoTAPc-TA-Au	$67.5^\circ \pm 1^\circ$	
CoTAPc-MPA-Au	$65.5^\circ \pm 1^\circ$	

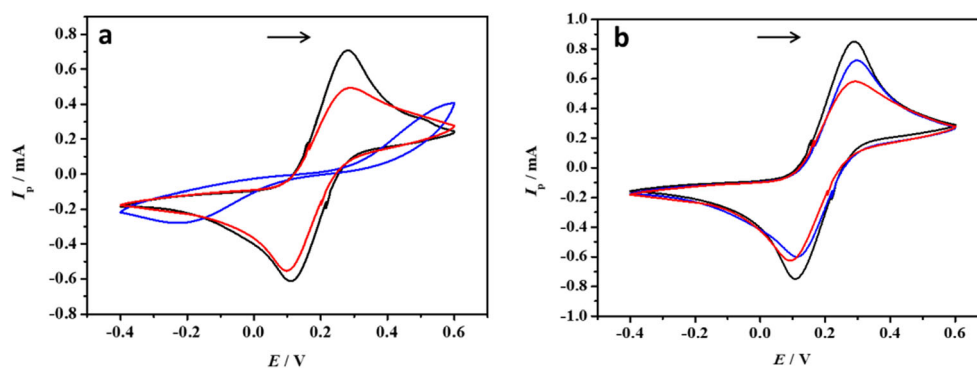
decrease in the CA values is expected, as the surface became more hydrophilic. The surface modified with TA shows less decrease in the CA value of the bare electrode compared to surface modified with MPA. The difference in the CA value between TA and MPA is attributed to the difference in the number of carbon atoms and the length of the molecules. After immobilization of CoTAPc in both cases, CA was increased to 67.5° and 65.5° for CoTAPc-TA-Au and CoTAPc-MPA-Au, respectively. Table 1 shows the contact angles at each step of electrode modification. Thus, as the prevention of the dissociation of organic ligands from the metallic surface and accordingly enhancing the SAM stability, is the prerequisite for the further application of it in electrochemical catalysis. Thioctic acid (TA) appears very promising for the stabilization and the further functionalization of SAM because it is characterized by a carboxylic acid group and two thiol functions, through which simultaneous anchorage onto a gold surface is possible. For the first time, we synthesized the phthalocyanine SAM on gold using TA for sensor application. The better stability of the dithiol TA constructed SAM on gold compared to the monothiol ligands of MPA constructed monolayer has been proved by experimental results which in close agreement with similar reports [35].

Electrochemical characterization

Cyclic voltammetry

Cyclic voltammetry (CV) is an electrochemical technique which measures the current that develops in an electrochemical cell under conditions where voltage is in excess of that predicted by the Nernst equation. It is a powerful and popular electrochemical technique commonly employed to investigate the reduction and oxidation processes of molecular species. CV is also invaluable to study electron transfer-initiated chemical reactions, which includes catalysis. CV is performed by cycling the potential of a working electrode, and measuring the resulting current. The gold electrode was scanned in $5 \text{ mmol L}^{-1} [\text{Fe}(\text{CN})_6]^{3-/4-}$ in $0.1 \text{ mol L}^{-1} \text{ KCl}$ solution between -0.4 and 0.6 V at a scan rate 0.1 V/s . As shown in Fig. 5a, the cyclic voltammogram recorded for the bare gold electrode shows an oxidation and reduction peaks that are related to the electron transfer processes between the gold electrode and ferricyanide solution with a peak separation $\Delta E = 163 \text{ mV}$. After immersing the bare electrode in thioctic acid solution, a monolayer was assembled and the electron transfer processes at the electrode surface was blocked which is an indication for a successful assembly process as the negatively charged carboxylic groups of the linker block the electron transfer processes with the negatively charged redox couple, very

Fig. 5 Cyclic voltammograms of gold electrodes (a) modified using TA (black: bare gold electrode; blue: TA-Au; red: CoTAPc-TA-Au) and (b) modified using MPA (black: bare gold electrode; blue: MPA-Au; red: CoTAPc-MPA-Au) in $5 \text{ mmol L}^{-1} [\text{Fe}(\text{CN})_6]^{3-/4-}$ in $0.1 \text{ mol L}^{-1} \text{ KCl}$ solution



weak oxidation and reduction peaks were observed and the peak separation increased, $\Delta E = 725 \text{ mV}$. After the chemical modification was applied for the carboxylic acid tail groups of thioctic acid by immobilizing the redox mediator CoTAPc via amide linkage using EDC coupling reagent and the electron transfer processes were resumed and the peak separation becomes $\Delta E = 174 \text{ mV}$ which is an indication for the success of the immobilization of the mediator. Figure 5(b) shows the CVs recorded for the modification of the gold electrode using mercaptopropionic acid (MPA) as the linking thiol, with $\Delta E = 174, 175$ and 187 mV for the bare gold, MPA-Au and CoTAPc-MPA-Au electrodes respectively, the electrochemical parameters of the Co(II)TAPc-modified gold electrodes using TA and MPA is summarized in Table S1.

Electrochemical impedance spectroscopy

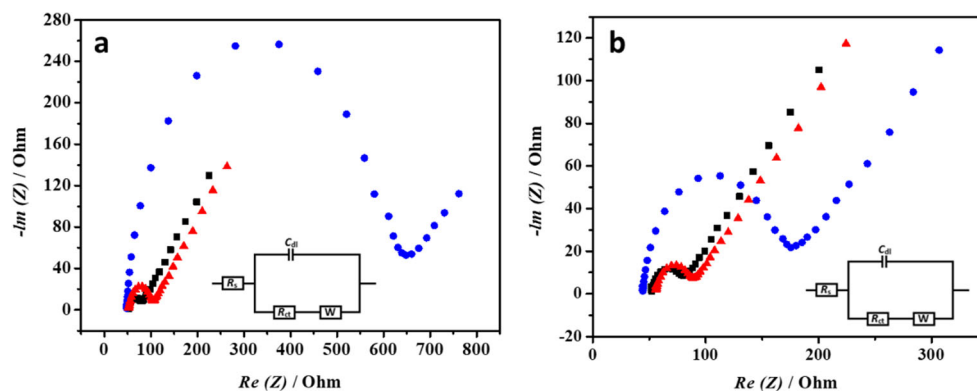
Electrochemical impedance spectroscopy (EIS) is an effective characterization technique for examining interfacial properties of modified electrodes. From the EIS measurements and equivalent electrical circuit designed from the impedance spectrum, R_{ct} values were calculated for each stage of electrode fabrication. The AC impedance of the gold electrode was recorded at different stages of its modification in $5 \text{ mmol L}^{-1} [\text{Fe}(\text{CN})_6]^{3-/4-}$ in $0.1 \text{ mol L}^{-1} \text{ KCl}$ solution at 0.24 V and frequency range from 0.1 Hz – 10^5 Hz as shown in Fig. 6(a, b). The obtained Nyquist plot shows a semicircle portion at higher frequencies corresponding to the electron transfer-limited process and a linear

part at the lower frequency range representing the diffusion-limited process. The semicircle diameter in the Nyquist plot is a measure of the charge transfer resistance (R_{ct}) and can be used to describe the interface properties at different stages of the electrode modification. R_{ct} directly affects the electron transfer process of the redox couple at the interface. The obtained data was fitted by applying an equivalent circuit for the system to get the R_{ct} values. The measured impedance, shown in Table S2, was found to be 564.1Ω and 121.8Ω for the TA/Au and MPA/Au electrode respectively. At the last step, CoTAPc was immobilized and onto both the TA and MPA functionalized gold electrodes where the impedance values of 46.69 and 30.89Ω for CoTAPc-TA-Au and CoTAPc-MPA-Au respectively were obtained. Thus, data in Table S2 reveals that formed TA and MPA thiols monolayer acts as a resistive layer due to the presence of negatively charged carboxylic groups which impede access of the anionic redox system compared to the bare gold electrode. The electrode surface modified with the CoTAPc redox mediator resulted in a significant reduction in R_{ct} indicating electron transfer accessibility and utility of the so formed catalytic film. EIS measurements shown in Table S2, was in agreement with the redox probe CV data above.

Electrode coverage rate

The electrode coverage (θ) is a key factor that can be used to estimate the surface state of the electrode and related to the resistance of the charge transfer. It is reasonable to assume that

Fig. 6 Nyquist plot of gold electrodes modified with (a) TA and (b) MPA (black: bare gold electrode; blue: thiol-modified Au; red: CoTAPc-modified Au) in $5 \text{ mmol L}^{-1} [\text{Fe}(\text{CN})_6]^{3-/4-}$ in $0.1 \text{ mol L}^{-1} \text{ KCl}$ solution, at 0.24 V from 0.1 to 10^5 Hz



highly compact and hydrophobic monolayers are practically insulating under usual electrochemical conditions, except in the existence of pinholes due to structural imperfections. Pinholes are a kind of defect in a thiol monolayer and they allow molecules and ions, from the electrolyte, reach the electrode surface. Assuming that all the current is passed by pinholes on the electrode, the electrode coverage can be calculated by the following equation:

$$\theta = 1 - \left(\frac{R_{ct}^{AuE}}{R_{ct}^{SAM}} \right)$$

Where θ is the coverage rate, R_{ct}^{AuE} is the charge transfer resistance of the gold electrode before functionalization, and R_{ct}^{SAM} is the charge transfer resistance after SAM formation. As per the calculations below, the coverage rate was found to be 0.96 and 0.80 for TA-Au and MPA-Au, respectively, as shown in Table S2. However, after immobilization the phthalocyanine, it was calculated to be 0.50 and 0.24 for CoTAPc-TA-Au and CoTAPc-MPA-Au, respectively. The high coverage of TA-Au electrode may be attributed to the fact that each molecule binds the gold surface by two Au-S bonds and this enhances the stability of the assembled layer. After immobilization, the surface coverage is still higher than that of MPA which again proves the stability due to strong binding of TA linker. Therefore, TA was chosen to prepare the modified electrode because of its strong binding with the surface and accordingly the CoTAPc is also more stable after immobilization [36, 37].

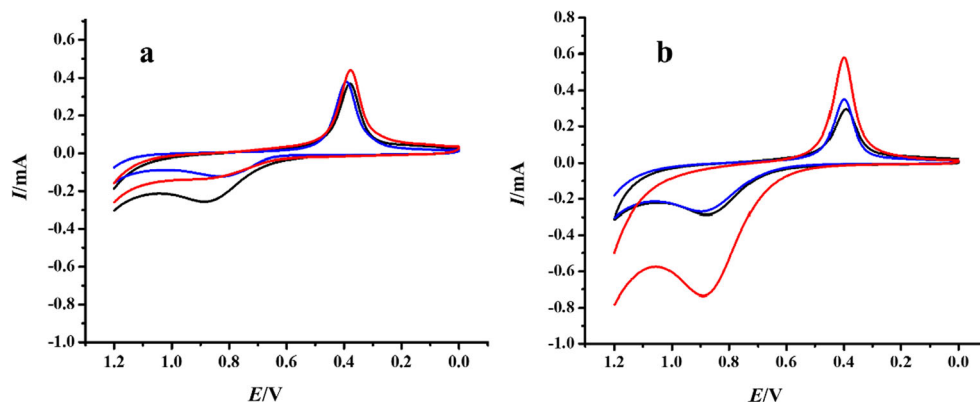
$$\theta(\text{TA-AuE}) = 1 - \left(\frac{23.4}{564.1} \right) = 0.96$$

$$\theta(\text{MPA-AuE}) = 1 - \left(\frac{23.6}{121.8} \right) = 0.80$$

$$\theta(\text{CoTAPc-TA-AuE}) = 1 - \left(\frac{23.6}{46.6} \right) = 0.50$$

$$\theta(\text{CoTAPc-MPA-AuE}) = 1 - \left(\frac{23.6}{30.9} \right) = 0.24$$

Fig. 7 Cyclic voltammograms of bare gold (black); TA-Au (blue); CoTAPc-TA-Au (red) electrodes in (a) absence of GSH and (b) presence of 25 mmol L⁻¹ GSH



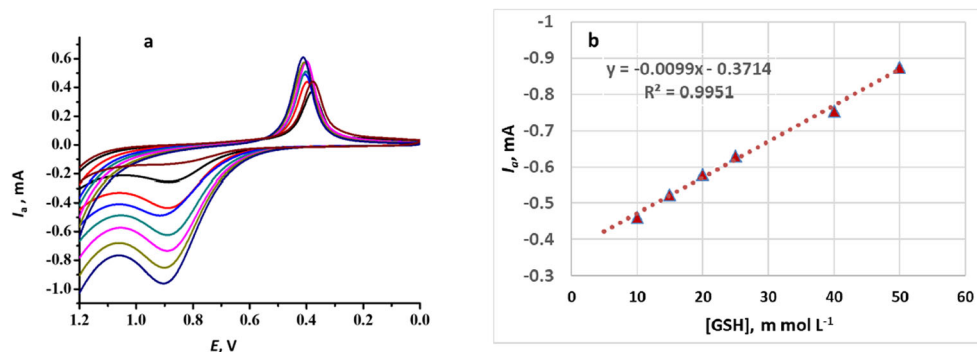
Electrochemical glutathione determination using CoTAPc-TA-Au electrode

Cyclic voltammetry

Cyclic voltammograms of bare gold electrode, TA-Au and CoTAPc-TA-Au in PBS in absence and presence of 25 mmol L⁻¹ GSH were recorded and shown in Fig. 7(a, b). It is obvious that the CoTAPc-modified electrode possessed the highest catalytic activity toward the oxidation of the GSH. Cyclic voltammograms of glutathione concentrations of 10, 15, 20, 25, 40, and 50 mmol L⁻¹ were recorded using the proposed CoTAPc-TA-Au electrode between 0.0 and 1.2 V in PBS of pH 7.4 at 100 mV s⁻¹ scan rate. As shown in Fig. 8(a), the oxidation peak is found to be at 888–904 mV and the reduction peak at 0.398–411 mV for the various GSH and GSSG concentrations respectively. Data in Table S3 reveals that as the GSH concentration increases the oxidation peak potential becomes more positive.

This is in agreement with a detailed study [38] which found that the reduction potential of the GSSG/2GSH half-cell is dependent on both the ratio of [GSH]/[GSSG] and the initial concentration of GSH. Their results revealed that the same ratios of [GSH]/[GSSG] will result in different reduction potentials as the concentration of GSH changes. On the other hand, diffusion is the random movement of molecules from a region of high concentration to regions of lower concentration. At low concentration of analyte, diffusion occurs in a satisfactory way, but at high concentration, the diffusion process is disrupted. In this condition, mass transport will be in trouble, so, compensation of these problems and re-establishment of mass transport, electrochemical system applies more potential; therefore, the peak potential will be shifted. As shown in Fig. 8(b), the resulting calibration graph of the oxidation peak current (I_a) vs. glutathione concentration exhibited a linear response over the concentration range between 10 and 50 mmol L⁻¹.

Fig. 8 (a) CVs of different glutathione concentrations (10, 15, 20, 40, and 50 mmol L⁻¹) in PBS using the proposed CoTAPc-TA-Au, pH = 7.4 and (b) the resulting calibration curve

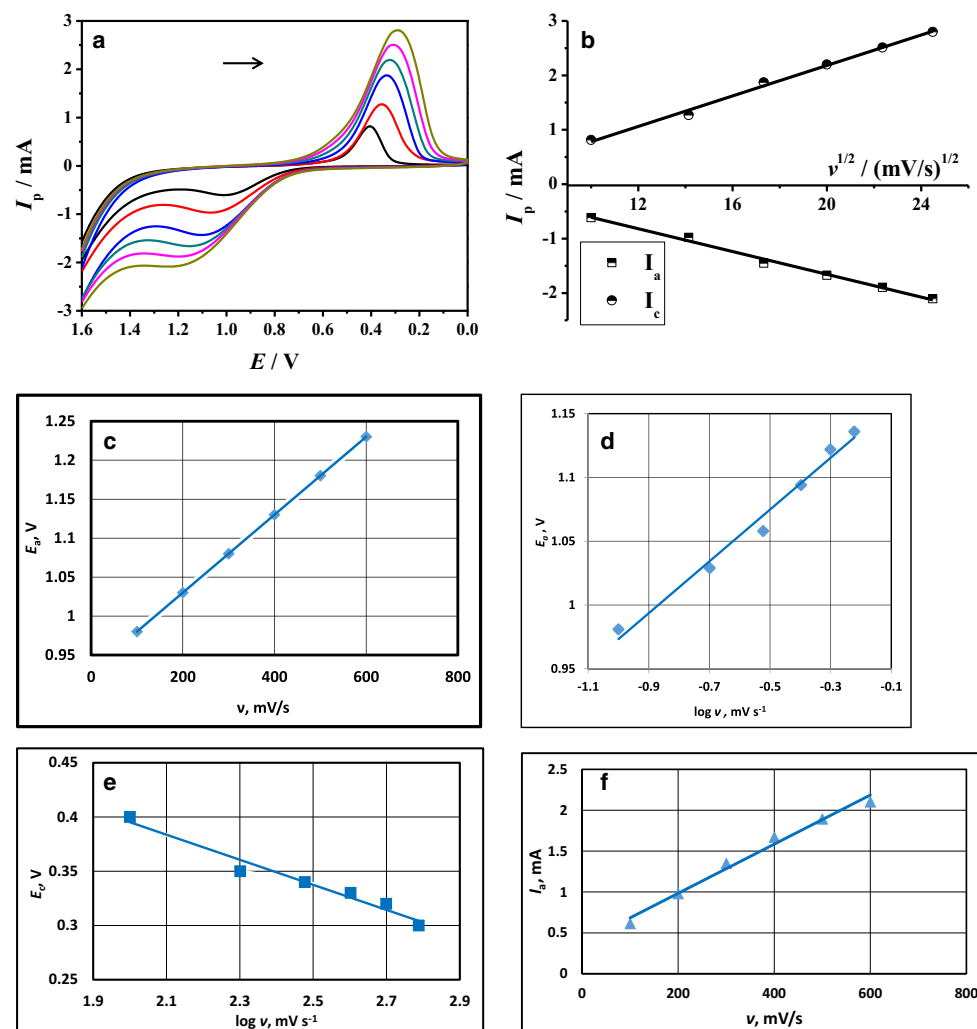


Effect of scan rate

Useful information involving electrochemical mechanism usually can be acquired from the relationship between the peak current and scan rate. Figure 9(a) shows the cyclic voltammograms of 25 mmol L⁻¹ of glutathione in PBS pH 7.4 recorded at the CoTAPc-TA-Au modified electrode at different scan rates in the range of 100–600 mV s⁻¹. From Fig. 9(b, c), it is obvious that the anodic and cathodic peak currents were in linear

dependences with the square root of the scan rate ($\nu^{1/2}$) in this range. The linear equation of both the reduction and oxidation peak currents versus $\nu^{1/2}$ are calculated as $y = 0.1401x - 0.6194$ ($R^2 = 0.9951$) and $y = 0.1047x + 0.4387$ ($R^2 = 0.9935$) respectively. As it is well known linear relationship between voltammetric peaks current (I_p) and square root of the scan rate ($\nu^{1/2}$) indicates diffusion controlled electrode kinetics. The graph of $E_p = f(\log \nu)$ yielded two straight lines with slopes of $-2.3RT/\alpha nF$ and $2.3RT/(1 - \alpha)nF$ for the cathodic peak and anodic peak,

Fig. 9 (a) Cyclic voltammograms of 25 mmol L⁻¹ glutathione in PBS at pH = 7.4 at different scan rates 100, 200, 300, 400, 500, and 600 mV/s; (b) The anodic and cathodic peak currents were in linear dependences with the square root of the scan rate in the range of 100–600 mV s⁻¹, (c) oxidation peak potential versus scan rate, (d) oxidation peak potential versus log scan rate, (e) reduction peak potential versus log scan rate, and (f) oxidation peak current versus scan rate



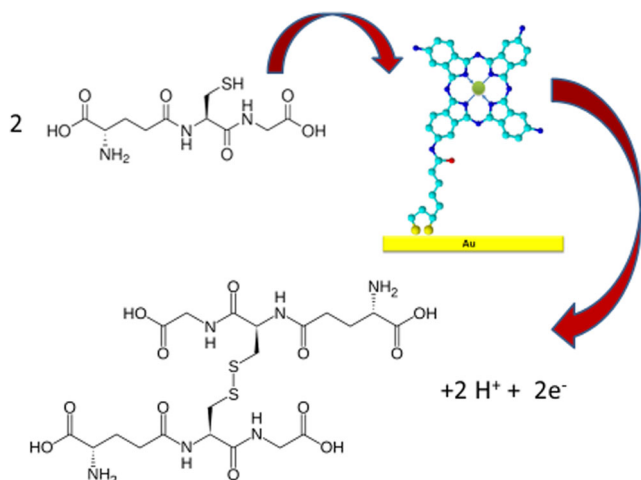


Fig. 10 Schematic presentation of the proposed mechanism

respectively (Fig. 9(d, e)), where α is the electron transfer coefficient, n is the number of electrons [39]. Thus, the value of α and n were estimated from the slopes of the straight lines to be 0.64 and 0.9 respectively, which indicate the rate determining step involve the transfer of one electron. In addition, the following Laviron equation [40] was used to calculate the value of the apparent heterogeneous electron transfer rate constant (k_s):

$$\log k_s = \alpha \log(1-\alpha) + (1-\alpha) \log \alpha - \log RT/nF\nu - \alpha(1-\alpha)nF\Delta E_p/2.3RT$$

where α is the electron transfer coefficient, n is the number of electrons, ΔE_p is the separation of the redox peaks, and ν is the scan rate. The electron transfer rate constant (k_s) was calculated to be 0.174 s^{-1} . Furthermore, Fig. 9(f) shows the linear plot of I_a vs. ν . From the slope the surface concentration of the electroactive species (Γ) can be estimated according to the following equation [41]:

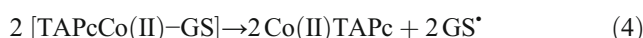
$$I_p = n^2 F^2 A \Gamma \nu / 4RT$$

Where, ν is the scan rate, n is the electron transfer numbers, F the Faraday number, A is the electrode surface area, R gas constant and T temperature. Γ was estimated to be $3.19 \text{ nmol cm}^{-2}$.

As shown also, it is clear that by increasing the scan rate, the peak potential is shifted to a more positive potential. The degree of surface coverage is a very important parameter in the construction of chemically modified electrodes (CMEs). Its value is strictly dependent on the surface morphology of the electrode. All the criteria affecting the electrochemical behavior of the mediator should be considered at the degree of surface coverage. As shown by increasing the scan rate, the peak potential is shifted to a more positive potential.

Mechanism

The mechanism of the electrocatalytic oxidation of GSH at the CoTAPc-modified gold electrode may be expressed as in the following Eqs. 1–5:



The proposed mechanism, (shown in Fig. 10), is in agreement with those previously reported [22, 42] and indicates that the first-one electron transfer is the rate-determining step for GSH oxidation.

Effect of pH

The effect of the solution pH on the electrochemical oxidation of GSH using 0.01 mol L^{-1} PBS at different pH values (6.8, 7, 7.4, 7.7, 8, and 8.5) was studied. The CoTAPc-modified gold electrode was scanned in 15 mmol L^{-1} glutathione in PBS at 100 mV s^{-1} . Figure 11(a) shows the cyclic voltammograms recorded for each pH and the peak current values were plotted against pH (Fig. 11(b)). The current increased with pH from 6.8 up to 7.4 and the current started to decrease by increasing

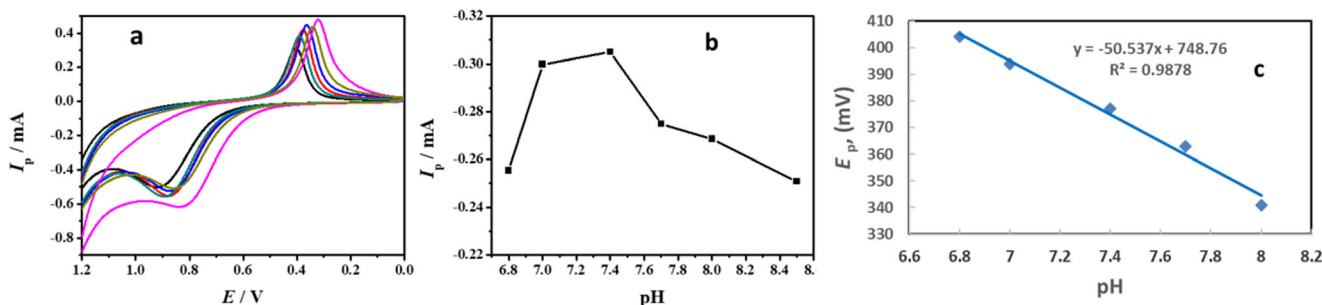


Fig. 11 (a) CVs of 15 mmol L^{-1} glutathione at scan rate 0.1 V/s and different pH values (6.8, 7, 7.4, 7.7, 8, and 8.5), (b) peak current values plotted against different pH, and (c) effect of pH on the oxidation peak potential

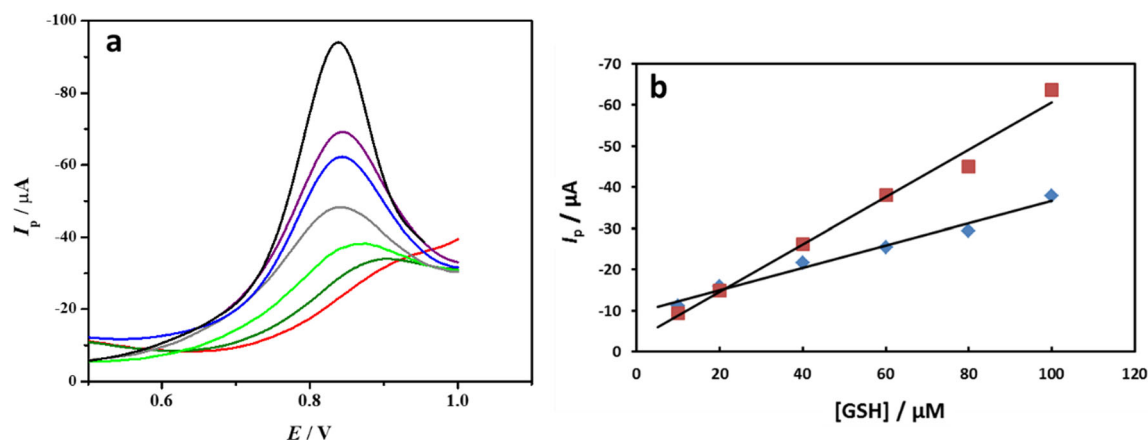


Fig. 12 (a) DPVs of glutathione concentrations of 0, 10, 20, 40, 60, 80, and 100 $\mu\text{mol L}^{-1}$ in PBS of pH 7.4 at CoTAPc-TA-Au and (b) the resulting calibration curves of both CoTAPc-MPA-Au (\blacklozenge) and CoTAPc-TA-Au (\blacksquare) modified electrodes using the same experimental parameters

the pH up to 8.5. The maximum current recorded was for pH 7.4 which is the physiological pH value at which the glutathione performs its action *in vivo*. The effect of pH on the peak potential was studied as well and the results show that by increasing the pH values the potential is shifted to lower values. The anodic peak potential of GSH at the surface of this modified electrode shifts to less positive values with increasing pH of the buffered solution as shown in Fig. 11(c). This negative shift in the anodic peak potential with pH indicates that the deprotonation step of GSH is prior to the electron transfer step [43]. It is also can be concluded according to Nernst equation and from the slope of the graph of E_p vs pH which is equal to -50.54 (which is close to the theoretical value 59.1) that one electron is involved in the electrochemical reaction.

Differential pulse voltammetry

Differential pulse voltammetry (DPV) is known to offer more sensitive measuring technique compared to the cyclic voltammetry. Figure 12(a) shows DPV for different concentrations of glutathione (10, 20, 40, 80, and 100 $\mu\text{mol L}^{-1}$), recorded by the modified electrodes (CoTAPc-TA-Au and CoTAPc-MPA-Au) in the range of 0.5 to 1.0 V in PBS (pH 7.4) at amplitude of 50 mV. The resulting peak potential and current for different glutathione concentrations using the proposed CoTAPc-TA-Au as well as data of the CoTAPc-MPA-Au electrodes are given in Table 2, for comparison purpose. Calibration graphs shown in Fig. 12(b) exhibit a linear response between oxidation peak current vs. glutathione concentration, over the concentration range between 10 and 100 $\mu\text{mol L}^{-1}$. The linear equation that represents the calibration lines are $y = -0.5751x - 3.1398$, $R^2 = 0.9869$ and $y = -0.2713x - 9.5448$, $R^2 = 0.9882$ for the two modified CoTAPc-TA-Au and CoTAPc-MPA-Au electrodes, respectively. The limit of detection (LOD) was calculated to be 1.5 and 5.5 $\mu\text{mol L}^{-1}$ GSH, respectively, with LOD defined as $3 S_b/$

m (where S_b is the standard deviation of the blank signal ($n = 3$) and m is the slope of the calibration curve).

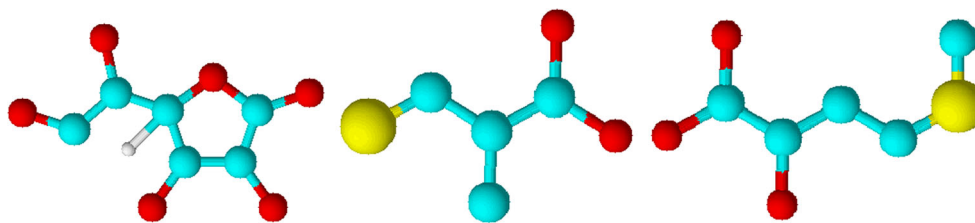
Interference study

The selectivity of the proposed sensor should be tested as we are aiming to apply this sensor to measure glutathione in real samples which contain some biologically important biomolecules and thiols that may interfere with glutathione determination. Figure 13 shows the interfering molecules ascorbic acid, methionine and cysteine that commonly present with glutathione in blood, which has been chosen for evaluating their effect on determination of glutathione in blood samples [20]. The optimum concentration of ascorbic acid is at the same concentration levels of glutathione [44]. But, concentrations of methionine and cysteine in plasma are double of the concentration of glutathione [45, 46]. The influence of these molecules was examined under the optimum conditions. Briefly, the percentage change in the current response of 50 $\mu\text{mol L}^{-1}$ glutathione was measured after addition of up to threefolds of ascorbic acid, methionine, and cysteine. The

Table 2 The DPV oxidation peak potential and current for different glutathione concentrations using both the CoTAPc-MPA-Au and CoTAPc-TA-Au modified electrodes

GSH, $\mu\text{mol L}^{-1}$	CoTAPc-MPA-Au I_a , μA	CoTAPc-MPA-Au E_a , mV	CoTAPc-TA-Au I_a , μA	CoTAPc-TA-Au E_a , mV
10	-11.2	884	-9.352	837
20	-15.97	880	-14.87	844
40	-21.59	872	-26.29	842
60	-25.39	868	-38.03	842
80	-29.31	856	-44.97	861
100	-37.92	836	-63.62	893

Fig. 13 The interfering molecules common present with glutathione in blood, ascorbic acid, methionine, and cysteine respectively



influence of these biomolecules on glutathione determination was measured as a percent recovery from the original current of glutathione prior to the addition of interferents (i.e., the oxidation peak currents were measured and correlated to the concentration ratio of each interferent, then, its percent contribution to GSH concentration was calculated). Table 3 shows the interference results for ascorbic acid, cysteine, and methionine. From these results, it is obvious that the contribution percent of ascorbic acid, methionine, and cysteine not exceeds 12.56%, 6.67%, and 9.05%, respectively.

The DPVs recorded for GSH, cysteine and their mixture in PBS, as well as the PBS alone using the modified electrode (CoTAPc-TA-Au), are shown in Fig. 14. It can be noticed that the position of oxidation peak of GSH at 0.85 V is far from that of cysteine which is located at 0.40 V. This is in agreement with data previously reported in literature, indicating that cysteine oxidation peak always appears around 0.5 V [20, 47–51]. The DPV recorded for 0.1 M PBS with zero concentration of both cysteine and glutathione (green curve) and that for cysteine in PBS with zero concentration of glutathione (red curve) showed a small broad peak around 0.9 V. This small peak can be attributed to the redox couple Co(II)/Co(III) of the phthalocyanine [37]. As well known, glutathione is a tripeptide with a gamma peptide linkage between the carboxyl group of the glutamate side chain and the amine group of cysteine, and the carboxyl group of cysteine is attached by normal peptide linkage to a glycine. The difference in oxidation peak position of glutathione and cysteine can be attributed to the difference in their structures which makes the oxidation of cysteine easier than that of the glutathione, so that the oxidation peak of cysteine appears at less positive potential. Also, it is clear from Fig. 14 that when the DPV was recorded for a mixture of glutathione and cysteine, only two oxidation peaks were observed at 0.83 V and 0.45 V without any overlap, where the peak of GSH at

0.83 V showed a little shift toward less positive potential value with a little increase in the current value.

A comparison of the performance of the proposed sensor to similar reports in the literature has been summarized in Table 4. It provides evidence of the analytical benefits obtained by the use of CoTAPc-modified gold electrode for glutathione determination. Data in table reveals that this work possesses a wide linear range and a good limit of detection when compared with previous reports. Recently, a nanocomposite molecular material based on cobalt phthalocyanine (CoPc) and multiwalled carbon nanotubes functionalized with carboxyl groups (MWCNTf) was developed for modifying glassy carbon electrodes (GCE) for the detection of reduced and oxidized glutathione [57]. The modified GCE showed that the combined use of CoPc and MWCNTf resulted in an electrocatalytic activity for GSH oxidation and GSSG reduction, enabling the simultaneous detection of both species. Differential pulse voltammetry allows obtaining detection limits of 100 μM for GSH and 8.3 μM for GSSG, respectively. However, in our work, a self-assembled monolayer (SAM) of cobalt teraaminophthalocyanine (CoTAPc) was developed on a thioctic acid (TA) dithiol modified gold electrode, thus the covalent binding of the phthalocyanine to the sensor matrix allowed for enhanced electrocatalytic performance of the developed glutathione (GSH) biosensor. Using the same DPV

Table 3 The effect of common interferents usually occur in blood on the determination of GSH by the proposed sensor

Interferent	Recovery, %		
	1:1	1:2	1:3
Ascorbic acid	93.25	92.46	87.44
Cysteine	102.85	107.39	110.95
Methionine	96.75	95.34	93.33

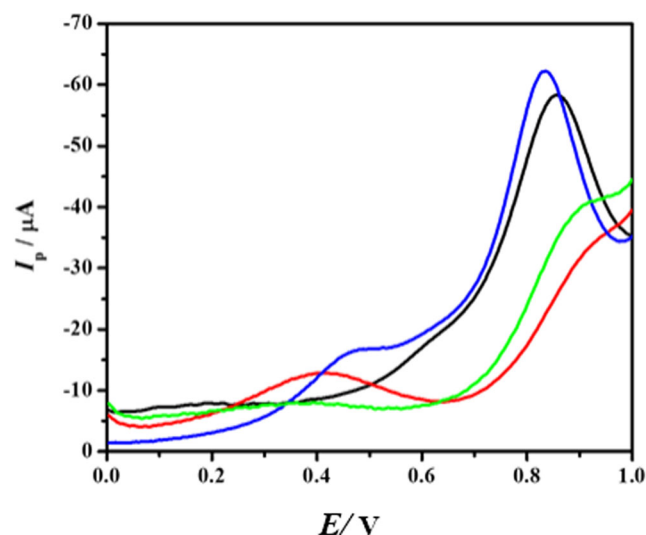


Fig. 14 DPVs recorded using the modified electrode (CoTAPc-TA-Au) in PBS pH 7.4 (green); 50 $\mu\text{mol L}^{-1}$ GSH (black); 50 $\mu\text{mol L}^{-1}$ Cysteine (red); Mixture of both (blue)

Table 4 Comparison of performance of the proposed CoTAPc-TA-Au gold sensor with previously reported sensors for the determination of GSH

Electrode material	LR ($\mu\text{mol L}^{-1}$)	LOD ($\mu\text{mol L}^{-1}$)	Ref.
Edge Plan Pyrolytic Graphite	10–80	2.7	[52]
Well-aligned CNTs	0.4–16.4	0.2	[53]
Glutathione peroxidase	19–140	15	[54]
Ceramic-CNT nanocomposite	–	20	[55]
Nitrosophenyl-modified carbon	–	8.1	[56]
CoPc/carboxyl groups modified MWCNT/ GCE	–	100	[57]
Co-based metal-organic coordination polymer	2.5–950	2.5	[58]
Co(II)TAPc-TA/Au	10–100	1.5	This work

technique, our developed sensor exhibited a linear response of oxidation peak current vs. GSH concentration, over the concentration range between 10 and 100 $\mu\text{mol L}^{-1}$ with a LOD of 1.5 $\mu\text{mol L}^{-1}$, with about 67 times better compared to the former composite-based sensor. It is worth mentioning that the amount of the apparent coverage calculated of the electroactive CoPc sites on the composite sensor was estimated to be $\Gamma = 3.33 \times 10^{-11} \text{ mol cm}^{-2}$, while for the SAM of CoPc in our developed sensor, Γ was estimated to be 3.19 nmol cm^{-2} , which is about two orders of magnitude higher, manifested in its higher sensitivity.

Real sample analysis

The standard addition method was used for glutathione determination. 0.1 mL of the prepared supernatant was added to 9.9 mL of 20 and 40 $\mu\text{mol L}^{-1}$ glutathione. The results are given in Table 5, which clearly demonstrate and confirm the capability of CoTAPc-modified gold electrode as suitable electrochemical sensor in the voltammetric determination of GSH.

Table 5 Glutathione determination in hemolyzed humane blood samples using the proposed sensor

GSH			
Sample	Added, $\mu\text{mol L}^{-1}$	Found, ($n = 3$) $\mu\text{mol L}^{-1}$	Concentration of real sample, mmol L^{-1}
1	0	14.8 ± 0.23	1.48
	20.0	33.5 ± 0.75	1.35
	40.0	56.0 ± 0.08	1.60
2	0	36.8 ± 0.91	3.68
	20.0	57.2 ± 0.34	3.72
	40.0	79.1 ± 0.17	3.91

Conclusions

The constructed cobalt phthalocyanine SAM on thioctic acid-modified gold electrode allowed for enhanced catalytic oxidation of reduced glutathione with minimum interference from ascorbic acid and cysteine, the compounds most probably occur with glutathione in blood. The assembled layer of CoTAPc-TA on the gold electrode was found to acquire more coverage rate compared to that constructed with MPA, allowing for improved sensitivity. Also, it was found to be strong enough to prolong the lifetime of the sensors due to the presence of two bonds between the gold surface and each molecule of the thiol linker. Thus, offering an excellent platform for formation of a more organized monolayer of CoTAPc which enhanced the oxidation of glutathione and allowed its sensitive determination in hemolyzed blood samples.

Acknowledgements The authors thank the EU for supporting this work through FP7 Marie Curie IRSES Project: Micro/nano sensors for early cancer warning system—diagnostic and prognostic information “SMARTCANCERSENS.”

Publisher's note Springer Nature remains neutral with regard to jurisdictional claims in published maps and institutional affiliations.

References

- Meister A, Anderson ME (1983) Glutathione. *Annu Rev Biochem* 52(1):711–760
- Giustarini D, Dalle-Donne I, Tsikis D, Rossi R (2009) Oxidative stress and human diseases: origin, link, measurement, mechanisms, and biomarkers. *Crit Rev Clin Lab Sci* 46(5-6):241–281
- Leonel C, Gelaleti GB, Jardim BV, Moschetta MG, Regiani VR, Oliveira JG, Zuccari DAPC (2014) Expression of glutathione, glutathione peroxidase and glutathione S-transferase pi in canine mammary tumors. *BMC Vet Res* 10(1):49–58
- Pastore A, Federici G, Bertini E, Piemonte F (2003) Analysis of glutathione: implication in redox and detoxification. *Clin Chim Acta* 333(1):19–39
- Townsend DM, Tew KD, Tapiero H (2003) The importance of glutathione in human disease. *Biomed Pharmacother* 57(3-4):145–155
- Rossi R, Dalle-Donne I, Milzani A, Giustarin D (2006) Oxidized forms of glutathione in peripheral blood as biomarkers of oxidative stress. *Clin Chem* 52(7):1406–1414
- Castejon AM, Spaw JA (2014) Autism and oxidative stress interventions: impact on autistic behavior. *Austin J Pharmacol Ther* 2:6–11
- Patel RS, Ghasemzadeh N, Eapen DJ, Sher S, Arshad S, Ko Y, Veledar E, Samady H, Zafari AM, Sperling L, Vaccarino V, Jones DP, Quyyum AA (2016) Novel biomarker of oxidative stress is associated with risk of death in patients with coronary artery disease. *Circulation* 133(4):361–369
- Toyo'oka T (2009) Recent advances in separation and detection methods for thiol compounds in biological samples. *J Chromatogr B* 877(28):3318–3330

10. Harfield JC, Batchelor-McAuley C, Compton RG (2012) Electrochemical determination of glutathione: a review. *Analyst* 137(10):2285–2296
11. Bai S, Chen Q, Lu C, Lin JM (2013) Automated high performance liquid chromatography with on-line reduction of disulfides and chemiluminescence detection for determination of thiols and disulfides in biological fluids. *Anal Chim Acta* 768:96–101
12. Schlereth DD, Katz E, Schmidt HL (1994) Toluidine blue covalently immobilized onto gold electrode surfaces: an electrocatalytic system for nadh oxidation. *Electroanalysis* 6(9):725–734
13. Willner I, Riklin A (1994) Electrical communication between electrodes and NAD(P)⁺-dependent enzymes using pyrroloquinoline quinone-enzyme electrodes in a self-assembled monolayer configuration: design of a new class of amperometric biosensors. *Anal Chem* 66(9):1535–1539
14. Collinson M, Bowden EF, Tarlov MJ (1992) Voltammetry of covalently immobilized cytochrome c on self-assembled monolayer electrodes. *Langmuir* 8(5):1247–1250
15. Duan C, Meyerhoff ME (1994) Separation-free sandwich enzyme immunoassays using microporous gold electrodes and self-assembled monolayer/immobilized capture antibodies. *Anal Chem* 66(9):1369–1377
16. Widrig CA, Chung C, Porter M (1991) The electrochemical desorption of n-alkanethiol monolayers from polycrystalline Au and Ag electrodes. *J Electroanal Chem* 310(1-2):335–359
17. Gatto E, Stella L, Formaggio F, Toniolo C, Lorenzelli L, Venanzi M (2008) Electroconductive and photocurrent generation properties of self-assembled monolayers formed by functionalized, conformationally-constrained peptides on gold electrodes. *J Peptide Sci* 14(2):184–191
18. Koufaki M, Detsi A, Kiziridi C (2009) Multifunctional lipoic acid conjugates. *Curr Med Chem* 16(35):4728–4742
19. Saeed AA, Singh B, Abbas MN, Issa YM, Dempsey E (2015) Electrocatalytic nitrite determination using iron phthalocyanine modified gold nanoparticles. *Electroanal* 27(5):1086–1096
20. Abbas MN, Saeed AA, Singh B, Radowan AA, Dempsey E (2015) A cysteine sensor based on a gold nanoparticle–iron phthalocyanine modified graphite paste electrode. *Anal Methods* 7(6):2529–2536
21. Mashazi PN, Ozoemena KI, Nyokong T (2006) Tetracarboxylic acid cobalt phthalocyanine SAM on gold: potential applications as amperometric sensor for H₂O₂ and fabrication of glucose biosensor. *Electrochim Acta* 52(1):177–186
22. Pereira-Rodrigues N, Cofré R, Zagal JH, Bedioui F (2007) Electrocatalytic activity of cobalt phthalocyanine CoPc adsorbed on a graphite electrode for the oxidation of reduced l-glutathione (GSH) and the reduction of its disulfide (GSSG) at physiological pH. *Bioelectrochem* 70(1):147–154
23. Xu H, Xiao J, Liu B, Griveau S, Bedioui F (2015) Enhanced electrochemical sensing of thiols based on cobalt phthalocyanine immobilized on nitrogen-doped graphene. *Biosens Bioelectron* 66:438–444
24. Hosseini H, Mahyari M, Bagheri A, Shaabani A (2014) A novel bioelectrochemical sensing platform based on covalently attachment of cobalt phthalocyanine to graphene oxide. *Biosens Bioelectron* 52:136–142
25. Wang X, Chen X, Evans DG, Yang WS (2011) A novel biosensor for reduced l-glutathione based on cobalt phthalocyaninetetrasulfonate-intercalated layered double hydroxide modified glassy carbon electrodes. *Sensors Actuators B Chem* 160(1):1444–1449
26. Honeychurch KC, Hart JP (2012) The chronoamperometric and voltammetric behaviour of glutathione at screen-printed carbon micro-band electrodes modified with cobalt phthalocyanine. *Adv Anal Chem Instrum* 2:46–52
27. Sehlotho N, Griveau S, Ruillé N, Boujtita M, Nyokong T, Bedioui F (2008) Electro-catalyzed oxidation of reduced glutathione and 2-mercaptoethanol by cobalt phthalocyanine-containing screen printed graphite electrodes. *Mater Sci Eng C* 28(5-6):606–612
28. NIST X-ray Photoelectron Spectroscopy Database, NIST Standard Reference Database 20, Version. 3.5, by C.D. Wagner, A.V. Naumkin, A. Kraut-Vass, <http://srdata.nist.gov>
29. Achar BN, Fohlen GM, Parker JA, Keshavayya J (1987) Synthesis and structural studies of metal(II) 4,9,16,23-phthalocyanine tetraamines. *Polyhedron* 6(6):1463–1467
30. Willey TM, Vance AL, Bostedt C, van Buuren T, Meulenberg RW, Terminello LJ, Fadley CS (2004) Surface structure and chemical switching of thioctic acid adsorbed on au(111) as observed using near-edge X-ray absorption fine structure. *Langmuir* 20(12):4939–4944
31. Matemadombo F, Westbroek P, Nyokong T, Ozoemena K, De Clerck K, Kiekens P (2007) Immobilization of tetra-amine substituted metallophthalocyanines at gold surfaces modified with mercaptopropionic acid or DTSP-SAMs. *Electrochim Acta* 52(5):2024–2031
32. Montalbetti CAGN, Falque V (2005) Amide bond formation and peptide coupling. *Tetrahedron* 61(46):10827–10852
33. Moulder JF, Stickle WF, Sobol PE, Bomben KD (1992) Handbook of X-ray photoelectron spectroscopy. Perkin-Elmer Corporation, Physical Electronics Division, Eden Prairie
34. Briggs D, Seah MP (1990) Practical surface analysis, 2nd edn. Wiley & Sons, Chichester
35. Fang Z, Liu L, Xu L, Yin X, Zhong X (2008) Synthesis of highly stable dihydrolipoic acid capped water-soluble CdTe nanocrystals. *Nanotech* 19(23):235603
36. Campuzano S, Pedrero M, Montemayor C, Fatás E, Pingarrón JM (2006) Characterization of alkanethiol-self-assembled monolayers-modified gold electrodes by electrochemical impedance spectroscopy. *J Electroanal Chem* 586(1):112–121
37. Braik M, Dridi C, Ali A, Abbas MN, Ben Ali M, Errachid A (2015) Development of a perchlorate sensor based on Co-phthalocyanine derivative by impedance spectroscopy measurements. *Org Electron* 16:77–86
38. Schafer FQ, Buettner GR (2001) Redox environment of the cell as viewed through the redox of the glutathione disulfide/glutathione couple. *Free Radic Biol Med* 30(11):1191–1212
39. Tian F, Gourine AV, Huckstepp RTR, Dale N (2009) *Anal Chim Acta* 645(1-2):86–91
40. Laviron E (1979) *J Electroanal Chem* 100(1-2):263–270
41. Prodromidis MI, Florou AB, Tzouvara-Karayanni SM, Karayannis MI (2000) The importance of surface covering in the electrochemical study of electrochemically modified electrodes. *Electroanal* 12(18):1498–1500
42. Gulppi MA, Páez MA, Costamagna JA, Cárdenas-Jirón G, Bedioui F, Zagal JH (2005) Inverted correlations between rate constants and redox potential of the catalyst for the electrooxidation of 2-aminoethanethiol mediated by surface confined substituted cobalt-phthalocyanines. *J Electroanal Chem* 580(1):50–56
43. Raoof JB, Ojani R, Baghayeri M (2009) Simultaneous electrochemical determination of glutathione and tryptophan on a nano-TiO₂/ferrocene carboxylic acid modified carbon paste electrode. *Sensors Actuators B* 143(1):261–269
44. Lenton KJ, Therriault H, Cantin AM, Fülöp T, Payette H, Wagner JR (2000) Direct correlation of glutathione and ascorbate and their dependence on age and season in human lymphocytes. *Am J Clin Nutr* 71(5):1194–1200
45. Chung JS, Haque R, Mazumder DNG, Moore LE, Ghosh N, Samanta S, Mitra S, Hira-Smith MM, von Ehrenstein O, Basu A, Liaw J, Smith AH (2006) Blood concentrations of methionine, selenium, beta-carotene, and other micronutrients in a case-control study of arsenic-induced skin lesions in West Bengal, India. *Environ Res* 101(2):230–237

46. Bridgeman MME, Marsden M, MacNee W, Flenley DC, Ryle AP (1991) Cysteine and glutathione concentrations in plasma and bronchoalveolar lavage fluid after treatment with N-acetylcysteine. *Thorax* 46(1):39–42
47. Singh M, Jaiswal N, Tiwari I, Foster CW, Banks CE (2018) A reduced graphene oxide-cyclodextrin-platinum nanocomposite modified screen printed electrode for the detection of cysteine. *J Electroanal Chem* 829:230–240
48. Hernández-Ibáñez N, Sanjuán I, Montiel MÁ, Foster CW, Banks CE, Iniesta J (2016) L-Cysteine determination in embryo cell culture media using Co(II)-phthalocyanine modified disposable screen-printed electrodes. *J Electroanal Chem* 780:303–310
49. Ziyatdinova G, Kozlova E, Budnikov H (2018) Selective electrochemical sensor based on the electropolymerized p-coumaric acid for the direct determination of L-cysteine. *Electrochim Acta* 270: 369–377
50. Kurniawan A, Kurniawan F, Gunawan F, Chou SH, Wang MJ (2019) Disposable electrochemical sensor based on copper-electrodeposited screen-printed gold electrode and its application in sensing L-Cysteine. *Electrochim Acta* 293:318–327
51. Premalatha S, Selvarani K, Bapu GNKR (2018) Facile electrodeposition of hierarchical co-Gd₂O₃ nanocomposites for highly selective and sensitive electrochemical sensing of L-cysteine. *ChemistrySelect* 3(9):2665–2674
52. Moore RR, Banks CE, Compton RG (2004) Electrocatalytic detection of thiols using an edge plane pyrolytic graphite electrode. *Analyst* 129(8):755–758
53. Tang H, Chen J, Nie L, Yao S, Kuang Y (2006) Electrochemical oxidation of glutathione at well aligned carbon nanotube array electrode. *Electrochim Acta* 51(15):3046–3051
54. Rover LR Jr, Kubota LT, Hoehr NF (2001) Development of an amperometric biosensor based on glutathione peroxidase immobilized in a carbodiimide matrix for the analysis of reduced glutathione from serum. *Clin Chim Acta* 308(1-2):55–67
55. Gong KP, Zhang MN, Yan YM, Su L, Mao LQ, Xiong SX, Chen Y (2004) Sol-gel-derived ceramic-carbon nanotube nanocomposite electrodes: tunable electrode dimension and potential electrochemical applications. *Anal Chem* 76(21):6500–6505
56. Abiman P, Wildgoose GG, Compton RG (2007) Electroanalytical exploitation of nitroso phenyl modified carbon-thiol interactions: application to the low voltage determination of thiols. *Electroanal* 19(4):437–444
57. Olmos Moya PM, Martínez Alfaro M, Kazemi R, Alpuche-Avilés MA, Griveau S, Bedioui F, Gutiérrez Granados S (2017) Simultaneous electrochemical speciation of oxidized and reduced glutathione. Redox profiling of oxidative stress in biological fluids with a modified carbon electrode. *Anal Chem* 89(20):10726–10733
58. Yuan B, Zhang R, Jiao X, Li J, Shi H, Zhang D (2014) Amperometric determination of reduced glutathione with a new Co-based metal-organic coordination polymer modified electrode. *Electrochem Commun* 40:92–95